Eur. Phys. J. D **9**, 491–494 (1999)

THE EUROPEAN PHYSICAL JOURNAL D

EDP Sciences

Magnetic dynamics of small α-Fe_2O_3 and NiO particles studied by neutron scattering

K. Lefmann[1], F. Bødker[2], M.F. Hansen[2], H. Vázquez[1,3], N.B. Christensen[1], P.-A. Lindgård[1], K.N. Clausen[1], and S. Mørup[2]

[1] Department of Condensed Matter Physics and Chemistry, Risø National Laboratory, DK-4000 Roskilde, Denmark
[2] Department of Physics, Building 307, Technical University of Denmark, DK-2800 Lyngby, Denmark
[3] Department of Physics, Universidad Autonóma de Madrid, Spain

Received: 1 September 1998

Abstract. We have studied the magnetic dynamics in nanocrystalline samples of α-Fe_2O_3 (hematite) and NiO by inelastic neutron scattering. By measuring around the structural and the antiferromagnetic reflections, we have probed uniform and staggered magnetic oscillations, respectively. In the hematite particles, we observed a clear double peak in the energy distribution of the antiferromagnetic signal, in addition to a quasi-elastic peak. We interpret the double peak to represent collective magnetic excitations. Broadening of the central quasi-elastic peak with increasing temperature is interpreted as a sign of superparamagnetic relaxation. Studies of the antiferromagnetic signal from NiO also show evidence of collective magnetic excitations, but with a higher energy of the precession states than for hematite. The inelastic signal at the structural reflection of NiO presents evidence for uniform magnetic oscillations very similar to the antiferromagnetic signal, as is expected for a simple antiferromagnet. The hematite sample did not show any signs of uniform oscillations, although these have been predicted theoretically.

PACS. 75.50.Tt Fine-particle systems – 76.60.Es Relaxation effects – 78.30.Nx Neutron inelastic scattering

1 Introduction

1.1 Magnetic fluctuations in nanosized particles

The study of magnetic fluctuations in small particles has attracted much attention. The problem is interesting from the point of view of both basic science and applications, e.g., in magnetic recording media [1]. In a single-domain ferromagnetic particle, the magnetization is often subject to a uniaxial anisotropy. This anisotropic energy may be approximated by

$$E_{\mathrm{an}} = K_{\mathrm{eff}} V \sin^2 \theta, \tag{1}$$

where θ is the angle between the magnetization and the easy axis, K_{eff} is the effective magnetic anisotropy constant, and V is the particle volume. At finite temperatures, thermally activated relaxation of the magnetization between the two energy minima (superparamagnetic relaxation) may take place. The characteristic relaxation time for this is described by the Néel–Brown theory [2], giving an Arrhenius-type law

$$\tau = \tau_0 \exp(K_{\mathrm{eff}} V / k_{\mathrm{B}} T), \tag{2}$$

where τ_0 is a characteristic attempt time (of the order 10^{-9}–10^{-12} s).

The particle magnetization may, however, also perform oscillations close to the easy directions. These collective excitations are related to long-wavelength spin waves. For small fluctuation amplitudes, (1) corresponds to the energy of a spin in an effective anisotropy field. In a classical description, this field leads to a precession of the particle moment, with a frequency of the order of 0.1 THz.

For antiferromagnets, the picture of magnetic oscillations and relaxations is still valid. One needs only to add the complication that there are two distinct sublattices, having coupled modes of oscillations in addition to the superparamagnetic relaxation. The magnetic anisotropy (1) should in this case be attributed to each of the sublattices.

The study of magnetic fluctuations in nanoparticles is usually carried out by ac and dc magnetization, covering fluctuation times in the ranges 10^4 to 10^{-5} s, or by Mössbauer spectroscopy, which is sensitive around 10^{-9} s. In order to study high-temperature superparamagnetic relaxation and collective excitations, we have employed inelastic neutron scattering, which is sensitive in the range 10^{-10} to 10^{-13} s. This method was first used for nanosized particles by Hennion *et al.* [3], who used elastic and inelastic scattering at small angles. In [4], we presented the first data on nanoparticles, obtained by the conventional triple-axis method. The present paper presents a continuation of the triple-axis work, applied to small particles of hematite (α-Fe_2O_3) and nickel oxide (NiO).

1.2 Magnetism of α-Fe_2O_3 and NiO

Bulk α-Fe_2O_3 is a two-sublattice antiferromagnet (AFM) at low temperatures, but above the Morin temperature, $T_M \approx 262\,K$, a small canting of the moments takes place to produce a weakly ferromagnetic (WFM) structure [5]. For small hematite particles, T_M is suppressed, and for our samples, the magnetic structure was WFM, down to at least 5 K. The moments are confined to the rhombohedral basal plane by a large anisotropy, which makes the spin system essentially two-dimensional [6].

Bulk NiO shows no Morin transition, and the structure is that of a simple AFM at all temperatures below the Néel temperature $T_N \approx 523\,K$ [7]. The Ni atoms are situated in a slightly distorted fcc lattice, in which the spins are ordered ferromagnetically within the (111) planes and antiparallel between adjacent planes (type II order). The spins are confined within the (111) planes, and the lattice distortion takes place in the direction perpendicular to these planes [7]. For very small NiO particles, the magnetic structure has recently been suggested to be a multisublattice structure [8].

One can identify two different long-wavelength modes for the collective oscillations of antiferromagnets: (i) the in-phase *uniform mode*, where the spins on different sublattices precess in phase, changing the angle between them, and (ii) the *staggered mode*, where the sublattices precess in precise antiphase, and in which the angle between the magnetization of the two sublattices is constant. These two fluctuation modes are illustrated for a ferromagnetic, an AFM, and a WFM system in Fig. 1.

Morrish has discussed the uniform and staggered precession modes in great detail for a general canted antiferromagnet [5]. For bulk WFM hematite, the uniform mode has a significantly higher energy than the staggered mode, the difference being about a factor of 2. Bulk NiO is a much less anisotropic antiferromagnet and, as such, is expected to show a degeneracy of the two modes. In small particles, the uniaxial anisotropy (1) does not change this property. Further, the behavior near the structural and antiferromagnetic Bragg peaks are also expected to be identical.

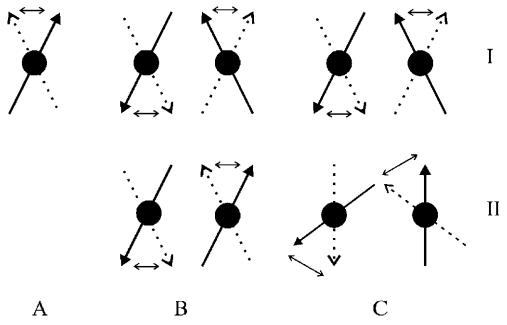

Fig. 1. Simplified fluctuation modes for (a) a simple ferromagnet, (b) a pure antiferromagnet such as NiO, and (c) a canted antiferromagnet such as hematite. The top row (I) shows the uniform modes, while the bottom row (II) displays the staggered modes.

2 Experiment

2.1 Sample preparation and characterization

The α-Fe_2O_3 sample was prepared by heating $Fe(NO_3)_3 \cdot 9H_2O$ in an oven at 90 °C [6]. The sample used in the neutron experiments had a mass of 5 g.

The NiO samples were produced by heating $Ni(OH)_2$ at various temperatures up to 500 °C. In this study, we present results from a 7 g sample treated at 300 °C.

Transmission electron microscopy revealed that the hematite particles were almost spherical in shape. The particles had a fairly broad size distribution: 10–25 nm [6]. In the same way, the NiO particles were found to be disk shaped, with a thickness of less than 2 nm, while the two other dimensions were typically 15 nm.

X-ray diffraction indicated that the mean particle size in the hematite sample was 15 ± 3 nm. Assuming a spherical particle shape, the mean particle size was found to be 5 ± 1 nm for the NiO sample.

Mössbauer spectra of the hematite sample indicated the presence of about 10% of impurities (ferrihydrite). These impurities were not found to be disturbing for the inelastic neutron measurements.

2.2 Inelastic neutron scattering

Neutrons are scattered by both nuclei and magnetic moments. The scattering cross sections are usually fairly small, and typical masses of powder samples are thus on the order of grams. Elastic neutron scattering yields information about the lattice structure and ordered magnetic structure, while inelastic neutron scattering is used for the study of lattice vibrations (phonons) and magnetic dynamics (spin waves, relaxation, etc.).

The magnetic neutron scattering cross section is given in terms of the neutron energy transfer, $\varepsilon = \hbar\omega$, and the neutron momentum transfer, $\hbar\boldsymbol{\kappa}$, by a double Fourier transform of the spin–spin correlation function [9]

$$\frac{\mathrm{d}^2\sigma}{\mathrm{d}\Omega\,\mathrm{d}E}(\boldsymbol{\kappa},\omega) \propto \int_{-\infty}^{\infty} \sum_{i,\alpha} \exp(\mathbf{R}_i \cdot \boldsymbol{\kappa} - \omega t)\, \langle s_0^\alpha(0) s_i^\alpha(t)\rangle \,\mathrm{d}t, \tag{3}$$

where s_i^α is the α $(= x, y, z)$ component of the spin (or, in general, the magnetic moment) on the ith atomic site. The spin may be decomposed into its time average, $\langle \mathbf{s}_i \rangle$, and its deviation from this, $\delta\mathbf{s}_i(t) = \mathbf{s}_i(t) - \langle \mathbf{s}_i \rangle$. In a semiclassical treatment, only the term $\langle \delta s_0^\alpha(0) \delta s_i^\alpha(t)\rangle$ of (3) contributes to the inelastic scattering ($\omega \neq 0$), while the term $\langle s_0^\alpha \rangle \langle s_i^\alpha \rangle$ gives rise to elastic scattering ($\omega = 0$). The two remaining terms vanish.

For a uniform precession mode, all spins precess in phase: $\delta\mathbf{s}_i = \delta\mathbf{s}_j$ for any i and j. Thus, the Fourier sum of (3) will peak at the lattice vectors corresponding to structural reflections. For a staggered precession mode, however, the Fourier sum peaks at the AFM ordering vector. The reason for this is that in the staggered mode,

$\delta\mathbf{s}_i = -\delta\mathbf{s}_j$ (as well as $\mathbf{s}_i = -\mathbf{s}_j$) when i and j are on different sublattices.

Let us now, for both modes of fluctuation, investigate the Fourier integral of (3). This provides the shape of the signal expected in an inelastic neutron scattering experiment where $\hbar\omega$ is varied, keeping $\boldsymbol{\kappa}$ constant. The energy line shape depends upon the nature of the relaxation mechanism: Superparamagnetic fluctuations are assumed to occur randomly, so that $\langle s_0^z(0)s_i^z(t)\rangle \propto \exp(-t/\tau)$, where z is taken as the easy axis. This leads to a Lorentzian energy line shape of width $\hbar/\tau$, centered at $\varepsilon = 0$. The collective magnetic excitations, on the other hand, give rise to peaks at $\varepsilon = \pm\varepsilon_0 = \pm\hbar\omega_0$, where ω_0 is the precession frequency. The neutron energy line shape thus reveals much information about the magnetic dynamics of small particles.

The measurements around the AFM ordering vector in hematite [4] were performed at the new high-performance RITA spectrometer at Risø [10], while the measurements around a structural reflection on hematite and all measurements on NiO took place on the Risø TAS7 spectrometer. Both experiments were performed using a conventional triple-axis setup. For all experiments, hard collimations were used in order to improve the energy resolution to the measured value (FWHM) of 0.070 meV at the RITA experiment, 0.155 meV for the TAS7 experiment around the AFM ordering vector in NiO, and 0.180 meV for the two experiments around the structural peaks.

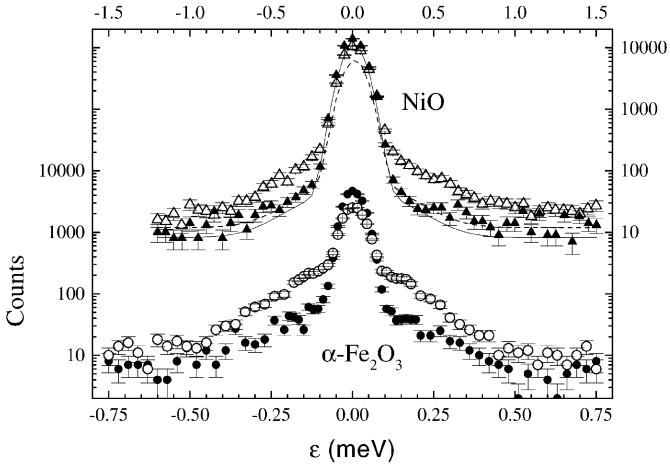

Fig. 2. Inelastic neutron scattering data around the antiferromagnetic reflections at temperatures of 50 K (filled data points) and 295 K (open data points). The top part of the figure represents NiO data at $\kappa = 1.30$ Å^{-1} (triangles), while the bottom of the figure is hematite data at $\kappa = 1.37$ Å^{-1} (circles). Fits to the background data for NiO ($\kappa = 1.60$ Å^{-1}) at 50 K are shown as the solid line; the dashed line shows the fit at 295 K. The energy transfer is given in units of 1 meV = 0.2418 THz. Note that the neutron counts are shown on a logarithmic scale and that the energy scale varies by a factor of 2 between the upper and lower data set.

3 Results

3.1 The staggered precession modes

Data showing the temperature and field dependences of the inelastic spectrum around the AFM ordering vector in hematite have earlier been published [4]. In order to compare with the other data presented, we show in Fig. 2 the zero field data for $T = 50$ K and for $T = 295$ K. The strong peak at zero energy transfer represents both the superparamagnetic signal and the incoherent elastic background, smeared out by the experimental resolution. The "shoulders" at about 0.2 meV are the expected signatures of collective magnetic excitations of the staggered precession modes.

The data were fitted to a model, which uses a sum of a Lorentzian contribution from the superparamagnetic relaxation, a damped harmonic oscillator function from the collective magnetic excitations, and an experimental background. All of this was convoluted with an (almost) Gaussian experimental resolution. A detailed study of the central peak reveals that its linewidth increases with temperature from 0.000(1) meV at 50 K to 0.011(2) meV at 295 K. The linewidth in the whole temperature range could be fitted to (2), giving $K_{\rm eff}V/k_{\rm B} = 500 \pm 200$ K and $\tau_0 \sim 7 \times 10^{-12}$ s [4]. The energy of the collective excitations was fitted to be $\varepsilon_0 = 0.26(2)$ meV at 50 K, decreasing to 0.205(5) meV at 295 K. This decrease is explained by the decrease of the effective anisotropy field with larger precession angle. In our first paper, we gave a value of $K_{\rm eff}V/k_{\rm B} = 1000 \pm 400$ K from the collective magnetic excitation data [4]. However, when the nearly two-dimensional nature of the hematite spin system is taken into account, this value is changed to $K_{\rm eff}^{\rm 2D}V/k_{\rm B} = 570 \pm 200$ K [6, 11], to be in better agreement with the other determination of the anisotropy.

Data showing the corresponding inelastic signal from our NiO sample at 50 K and 295 K are presented in Fig. 2. The data at room temperature show a clear enhancement around $\varepsilon = 0.5$ meV, although the shoulders are much broader than in the hematite data. We have fitted the data to the same model as was used for the hematite data. For the room temperature data, the excitations have an energy of $\varepsilon_0 = 0.43(6)$ meV, a factor of 2 higher than for hematite, while the damping factor is enhanced even more: $\Gamma = 0.4(1)$ meV, as compared with 0.13(1) meV for hematite. Fits to the low temperature data did not reveal any contributions from collective magnetic excitations. With the present experimental resolution, we were not able to see any broadening of the central peak, although this is expected from superparamagnetic relaxation in NiO.

3.2 The uniform precession modes

Inelastic neutron data taken at two temperatures at the two samples at a κ value corresponding to a structural reflection are shown in Fig. 3. The background measurements at room temperature are seen to have rather high values even far from the central peak as compared to the data presented in Fig. 2. This partly obscures the presence of a temperature-dependent signal from the NiO sam-

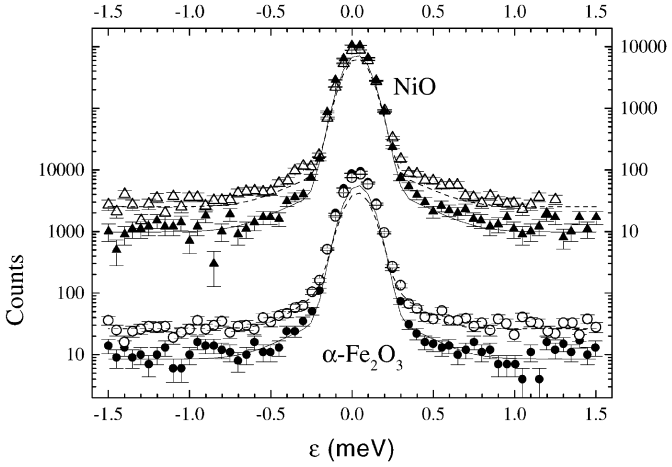

Fig. 3. Inelastic neutron scattering data around a structural reflection at temperatures of 10 K (filled symbols) and 295 K (open symbols). The upper part of the figure shows the NiO data (triangles) taken at $\kappa = 2.55\,\text{Å}^{-1}$, while the lower part shows the data for hematite (circles) taken at $\kappa = 2.35\,\text{Å}^{-1}$. Fits to the background data at 10 K and 295 K are shown as solid and dashed curves, respectively. The background data were taken at $\kappa = 2.00\,\text{Å}^{-1}$ for NiO and $\kappa = 2.60\,\text{Å}^{-1}$ for hematite.

ple. This signal was fitted to the model described earlier, giving the following values for the collective magnetic excitations at room temperature: $\varepsilon_0 = 0.46(9)$ meV and $\Gamma = 0.5(1)$ meV. The total area of this signal is 0.7(3) times that of the similar signal taken at the AFM κ value.

Similar data for hematite are presented in Fig. 3. No data points are significantly above background, and no damped harmonic oscillator signal is revealed by the fitting.

4 Discussion

From both samples, we have seen a clear inelastic signal at the AFM κ values, and the signal increases with temperature. The same is true for the NiO sample at the structural κ value. ε_0, Γ, and the signal intensity do not seem to vary significantly between the two data sets. This is in good agreement with our understanding of NiO as being a simple antiferromagnet. We thus interpret our observations as a strong indication of the existence of thermally agitated uniform and staggered collective magnetic excitations in NiO. The large observed broadening of the excitation signal in NiO (and to some extent in hematite) could be attributed either to damping of the collective oscillations by particle–particle interactions or to a distribution of precession frequencies due to variations in, e.g., the magnetic anisotropy.

To our surprise, no inelastic signal above background is seen at the structural κ value for hematite within $\varepsilon = \pm 1.5$ meV, although a uniform oscillation mode is expected from bulk data to be present at $\varepsilon_0^{\text{u}} \approx 0.4$ meV. This could be explained by a large increase of ε_0^{u} in nanosized particles as compared to the bulk value, or by a reduction of the intensity relative to the staggered precession mode, making the signal too small to observe in the present experiment.

In the work shown here and in our previous paper [4], we have demonstrated that it is feasible to study both superparamagnetic relaxation and collective magnetic excitations in antiferromagnetic materials using inelastic neutron scattering. However, neutron investigations of nanosized particles are by no means limited to the techniques or to the materials presented here. Despite the requirement for large sample masses, the use of neutron scattering as a tool for studying the magnetism of nanoparticles may prove to be of much value in the future.

References

1. see, e.g., J.L. Dormann, D. Fiorani (Eds.): *Magnetic Properties of Fine Particles* (North-Holland, Amsterdam 1992)
2. L. Néel: Ann. Geophys. **5**, 99 (1949); W.F. Brown, Jr.: Phys. Rev. **130**, 1677 (1963)
3. M. Hennion *et al.*: Europhys. Lett. **25**, 43 (1994)
4. M.F. Hansen *et al.*: Phys. Rev. Lett. **79**, 4910 (1997)
5. A.H. Morrish: *Canted Antiferromagnetism: Hematite* (World Scientific, Singapore 1994)
6. F. Bødker *et al.*: to appear in Phys. Rev. B (2000)
7. W.L. Roth: Phys. Rev. **110**, 1133 (1958)
8. R.H. Kodama, S.A. Makhlouf, A.E. Berkowitz: Phys. Rev. Lett. **79**, 1393 (1997)
9. See, e.g., G.L. Squires: *Introduction to the Theory of Thermal Neutron Scattering* (Cambridge University Press, Cambridge 1978)
10. T.E. Mason *et al.*: Can. J. Phys. **73**, 697 (1995); K.N. Clausen *et al.*: Physica B **241–243**, 50 (1998)
11. M.F. Hansen: *Magnetic Properties of Systems of Magnetic Nanoparticles* (Ph.D. thesis, Technical University of Denmark, 1998)